K-N S channel $I=1,0$ phase shifts as a direct measure of chiral condensation

P. Bicudo, J. Ribeiro, and J. Rodrigues
Instituto Superior Tecnico, Avenida Rovisco Pais, 1100 Lisboa Codex, Portugal
(Received 7 November 1994)

We study, in the framework of a QCD-inspired confining Nambu–Jona-Lasinio model, the $I=1;0$, S-wave K-N phase shifts for simple examples of chirally consistent microscopic potentials. The Dyson equation for the scattering of the bound states K and N is solved. The equivalence between this equation and the resonating group method equation is presented. The role of the chiral symmetry in the strength of the effective hyperfine potential, simultaneously responsible for the features of K-N repulsion and the $\pi-\rho$ mass difference, is discussed.

PACS number(s): 24.85.+p, 12.39.Fe, 12.39.Pn, 13.75.Jz

I. INTRODUCTION

The studies of the K-N reactions have a long history dating back to the 1950s. Already, in 1953, Chew [1] realized that it was absolutely necessary to spread out the region of interaction (between a pion and a nucleon), or in other words to introduce a cutoff in momentum space of the order of 450 MeV, if he was ever going to have meaningful results for the π-proton cross section. With the prequark knowledge of the time this cutoff was interpreted as an effective simulation of a mixture of nucleon recoil effects together with something else which rendered the theory nonlocal. Four years later this theory was extended to the study of low-energy scattering of K^+ particles by nucleons [2]. In this Chew-theory approach for the K-N interactions one had a vertex described as a direct product of a gradient coupling $\sigma\cdot\mathbf{k}$ in ordinary spin space and an isotopic nucleon-kaon-hyperon vertex. In the same year Schwinger [3] introduced a new scalar meson σ which, in conjuction with the V-A theory of the β decay and the Feynman-Gell-Mann [4] universality hypothesis for the V-A theory, motivated a series of articles on chiral symmetric Lagrangians for nucleons and pions in terms of the phenomenological π-N coupling constants and the intervening hadronic masses [5]. These Lagrangians were built in such way as to have a mechanism of spontaneous breaking of chiral symmetry which was held responsible for the partial conservation of the hadronic axial current (PCAC). Quarks were introduced in 1964 [6], and this prompted 30 years of quark hadronic spectoscopy, up to the present day, basically along two main lines which can be summarized under the names of the naive quark model (NQM) and bag model (BM).

The bag model story started with Bogolioubov [7] in the late 1960s. Conservation of the energy momentum tensor for the confined quarks led to the introduction of a phenomenological bag energy density together with a Lagrange multiplier of the type q-$\bar{q}$ at the confining bag surface. This last term breaks chiral symmetry and soon it was realized [8] that pions, as a fundamental field, should be coupled to the bag surface if we were to have a chiral-invariant Lagrangian for the bag model. The final step which led to the formulation of the cloudy bag model (CBM) [9] was the recognition that the quarks themselves should be dressed with pions and in this way the pions were allowed inside the bag. By simple inspection of the obtained Lagrangian it was then possible to rederive the Weinberg-Tomozawa result for soft-pion-hadron scattering lengths [10]. The CBM prompted a wealth of papers on pion-nucleon scattering [11] as well as on K-N scattering [12]. The main conclusions were that a qualitative agreement with the K-N experimental phase shifts was possible for a bag radius around 1 fm. This short summary illustrates the connection existing between confinement, chiral symmetry, and soft pion- (and kaon-) -hadron cross sections. Naturally it is to be expected that this connection will continue to play a major role in any quark microscopic, chiral-invariant, effective Lagrangian, with pions as q-$\bar{q}$ bound states instead of as pointlike particles.

As for the NQM, notwithstanding its considerable phenomenological success, it fails to accomodate in a simple way the requirements of spontaneous breaking of chiral symmetry, i.e, PCAC. The solution of this inadequacy goes along the lines first proposed, in analogy with the BCS theory [13] of superconductivity, by Nambu and Jona-Lasinio [14] in the framework of a Lagrangian with nucleons and pions. The same theory can be formulated in terms of quarks and a QCD-inspired quark microscopic potential and has been pursued by several authors [15–20]. In what concerns the non-exotic reactions, like for instance π-N reactions, where quark-antiquark annihilation plays a crucial role in the π-N kernel, allowing for the S-channel exchange of three-quark baryonlike intermediate states, these types of theory lead to a picture that, when seen as an effective meson-nucleon theory, looks like the Chew theory, with effective K-N-hyperon vertices and a cutoff naturally provided by the smallest size of the intervening hadrons.

Exotic reactions like those studied in the present work, where the antiquark $\bar{s}$ cannot annihilate with any of the quarks intervening in the reaction, essentially involve five-quark irreducible amplitudes without s-channel resonances, which then can be thought as an effective K-N-K-N vertex which lies outside Chew theory. This is one of the reasons why, to our knowledge, the K-N exotic S-channel $I=1$, 0 phase shifts have not yet been theoretically understood. This is the more striking as these phase shifts provide a demanding test for the effective microscopic q-q potential. K-N scattering, being exotic on one hand, that is, without S-channel q-$\bar{q}$ annihilation amplitudes, and on the other hand having no T-channel exchange of pions (because of G parity), should constitute a "clean" reaction, to be described solely in terms of overlap kernels and the microscopic quark forces. In this respect K-N scattering is much simpler to study than the π-N reaction which is nonexotic; i.e., it possesses extra quark-antiquark annihilation amplitudes (which are also naturally present in the Hamiltonian) on top of those quark-antiquark scattering amplitudes already contributing in K-N. It happens that these annihilation amplitudes do not contribute to the K-N scattering amplitude. Second, in K-N reactions we do not have to take into account the quasi-Goldstone pion characteristics, which differ from the kaon in one crucial point. The reactions where the kaon participates can be well described with just one Salpeter amplitude for the kaon (the so-called positive E-spin amplitude), the negative E-spin contribution being much smaller ($\sim 10\%$). The same considerations do not apply to the pion. Its negative E-spin Salpeter amplitude is similar in strength to the positive E-spin amplitude and in this case we had to take into account, just for the diffractive part, at least four different π-N amplitudes instead of just one in the case of K-N scattering. Finally, as consequence of the quark-antiquark annihilation amplitudes, we still have to consider the intermediate s-channel N resonance in order to have an "accurate" picture of the physics involved in π-N scattering, which we can see to be clearly more complicated than the K-N reaction. More generally, in hadronic reactions the strong influence of the mechanism of spontaneous chiral symmetry breaking is self-consistently exerted in two separate sectors: in the asymptotic Salpeter amplitudes of the intervening hadrons and in the effective modifications it introduces in the quark-quark microscopic potential. In K-N scattering, due to the presence of a strange quark, the former of these two sectors is rendered trivial and we therefore could concentrate on the effects of chiral symmetry breaking in the microscopic potential. Once this study done, we could then turn to the effect of more complicated Salpeter amplitudes; that is, we can go from the kaon to the pion. In this respect, the present calculation can be regarded as a stepping stone to the more elaborate π-N calculation.

Because the overlap kernel contributions to the total K-N force get mixed with the q-q force, it is important to be able to disentangle these two types of contributions in order to isolate quark dynamics from the "Pauli forces." For this purpose we used some years ago [15] a general method which allowed for the separation between dynamics and these geometrical overlaps. This method allowed for a systematic study of, at that time, popular quark potentials [21]. The conclusions were that K-N phase shifts could not be explained by the interplay between the Pauli principle and quark-quark interactions fitted to the spectroscopic sector. Not only did the sizes of the intervening kaon and nucleon turn out to be too big but also the strength of the microscopic hyperfine force appropriate to fit the hadron spectroscopy was much larger than needed to describe the K-N repulsion. Therefore, if we insisted in getting the spectroscopy right, we got far too much K-N repulsion. Conversely, if we fixed the K-N repulsion, we got, in the framework of an effective nonrelativistic Hamiltonian, hyperfine splittings which were much too weak. All in all the naive quark model (NQM) K-N phase shifts were bad. Of course it was known that the physical nucleon had more to it than to be a simple three-valence-quark bound state. The $N\pi$ and $\Delta\pi$ virtual channels were bound to force down whatever three-quark nucleon bare mass we found which in turn meant that this mass ought to be larger than 938 MeV [22]. And a larger bare mass would have implied a small bare nucleon size. How big should this mass be we could not really know because in the NQM we cannot theoretically treat quark-antiquark pair creation or have (in the same theory) any means to describe the pion.

As we already said this failure of the constituent quark models could be anticipated because all these models miss the physics of spontaneous chiral-symmetry breaking (χ SB) which is a basic tenet of strong interactions. From the point of view of χ SB the K meson does not differ too much, with the notable exception of its negative energy component, from the quasi-Goldstone pion and therefore it is only natural to expect the chiral condensate to influence the K-N phase shifts, this being mainly due to the presence in the kaon of a light quark. In fact it is a double influence because the physics of chiral symmetry also forces the nucleon to be far from being a simple three-quark bound state squeezed as it is by a pion cloud (which is largely invisible to the K meson because of G parity). In other words the kaon will act as a probe for the bare nucleon component of a multichannel physical nucleon. Therefore because the size of the participating hadrons is important in the evaluation of phase shifts, we must resort to a specific field-theoretical model if we want to study the K-N scattering. At this stage and in order to better understand the physical issues involved, extracting them from a background of already quite extensive calculations, we feel that it is important and perhaps essential to study relatively simple dynamical models not only consistent with the requirements of χ SB, but still able to give a fair spectroscopy of light mesons. Furthermore, in these models it is quite easy to turn on and off the mechanism responsible for the χ SB, and to see whether, and how much, this affects the phase shifts. Finally, we still have to compare several such models in order to distinguish the general physical issues from the particular details of a given model. For this matter we considered the cases of the harmonic and linear confining quark potentials. By contrasting the results of these two cases, we could understand the K-N phase shifts in terms of two simple (and related) parameters: the size of the bare nucleon and the extent of the chiral condensate. With χ SB on, the K-N phase shifts turn out to improve substantially over those obtained in the NQM. On the other hand, if we turn off the χ SB, we see a dramatic change in the K-N phase shifts. We organize the remainder of this paper in five sections and three appendixes. Section II is devoted to a brief description of the microscopic model we will be using. In Sec. III we introduce the Dyson Bethe-Salpeter equations both for mesons and baryons consistent with spontaneous chiral symmetry breaking. Next, in the Sec. IV, we discuss the derivation of the resonating group method and its application to th K-N scattering. In the last section we present and discuss the results. Finally we have three appendixes which contain the material needed for Sec. IV. Appendix A is devoted to outline the derivation of the resonating group method (RGM) equation from the Dyson series for the K-N S matrix [16]. In Appendixes B we discuss the evaluation of the spin-flavor overlaps [15] and in Appendix C we present the graphical rules [23], necessary for the evaluation of space overlaps.

II. QUARK MODEL WITH CHIRAL SYMMETRY BREAKING

The microscopic quark forces we will be using have been extensively studied [17,18,20]. Here we present the basic ingredients of the model. First let us introduce the Hamiltonian of the model which is

$$H=\int d^3x[H_0(\mathbf{x})+H_I(\mathbf{x})] \quad , \tag{1}$$

where H_0 is the Hamiltonian density of the Dirac field, and H_I an effective interaction term,

$$H_0(\mathbf{x})=\psi^\dagger(\mathbf{x})(m_q\beta-i\vec{\alpha}\cdot\vec{\nabla})\psi(\mathbf{x}),$$

$$H_I(\mathbf{x})=\tfrac{1}{2}\int d^3y\; V_I(\mathbf{x}-\mathbf{y})\bar{\psi}(\mathbf{x})\frac{\lambda^a}{2}\gamma^0\psi(\mathbf{x})\bar{\psi}(\mathbf{y})\gamma^0 \times\frac{\lambda^a}{2}\psi(\mathbf{y}) \quad . \tag{2}$$

The λ^a's are the Gell-Mann color matrices. For $V_I(\mathbf{x}-\mathbf{y})$ we study both the harmonic and linear confining potentials:

$$\begin{array}{lll} & \text{harmonic} & \text{linear} \\ V(\mathbf{x}) & =K_H^3\mathbf{x}^2, & K_L^2|\mathbf{x}|. \end{array} \tag{3}$$

With these choices, partly motivated for calculational simplicity, we still obtain a not too unreasonable charmonium and bottomonium spectroscopy while being able to keep the masses of the π, ρ, and the K meson at their physical values [17,18,19]. In Eq. (2), the field operator $\psi_{fc}(\mathbf{x})$ is defined as,

$$\psi_{fc}(\mathbf{x})=\int \frac{d^3p}{(2\pi)^{3/2}}[u_s(\mathbf{p})b_{fsc}(\mathbf{p})+v_s(\mathbf{p})d^\dagger_{fsc}(-\mathbf{p})]e^{i\mathbf{p}\cdot\mathbf{x}} \quad . \tag{4}$$

b and d are, respectively, the quark and antiquark Fock space operators and they carry indices for flavor, spin, and color. Summation over repeated indices is used throughout this paper. The spinors u and v and the Fock space operators differ from those used in free Dirac theory. For u_s and v_s we have

$$u_s(\mathbf{p})=\frac{1}{\sqrt{2}}\{[1+\sin\varphi(p)]^{\frac{1}{2}}+[1-\sin\varphi(p)]^{\frac{1}{2}}\hat{\mathbf{p}}\cdot\vec{\alpha}\}u_s^0 \quad ,$$

$$v_s(\mathbf{p})=\frac{1}{\sqrt{2}}\{[1+\sin\varphi(p)]^{\frac{1}{2}}-[1-\sin\varphi(p)]^{\frac{1}{2}}\hat{\mathbf{p}}\cdot\vec{\alpha}\}v_s^0, \tag{5}$$

where u_s^0 and v_s^0 are spinor eigenvectors of γ_0 corresponding to eigenvalues ± 1. The function $\varphi(p)$ is called the *chiral angle* and indexes the different Fock spaces compatible with the Pauli principle. This chiral angle has been studied in Refs. [17,18]. It should be stressed that in the limit of zero current quark mass and zero potential (which means $\varphi=0$), expression (5) yields the usual massless Dirac spinors whereas for massive fermions and for all momenta small enough we have $\varphi=\pi/2$, and, for this region of momentum, Eq. (5) becomes a formal identity.

It is worthwhile to digress a little on the physics behind chiral symmetry spontaneous breaking which hinges essentially on this liberty we have in choosing the fermion Fock space. It turns out that the Hamiltonian defined in Eqs. (1) and (2) is invariant (for $m_q=0$) under the global symmetry, involving γ_5:

$$\Psi\rightarrow\exp(-i\alpha^aT^a\gamma_5)\Psi, \quad \bar{\Psi}\rightarrow\bar{\Psi}\exp(-i\alpha^aT^a\gamma_5). \tag{6}$$

To this symmetry we associate the axial charge Q_5^a,

$$Q_5^a=\int d^3x\;\bar{\Psi}\gamma_0\gamma_5T^a\Psi. \tag{7}$$

Now, using the spinors of Eq. (5) we obtain, for the axial charge,

$$\begin{aligned} Q_5^a=\int d^3p\sum_{ss'} & \cos\varphi(p)(\vec{\sigma}\cdot p)_{ss'}b^\dagger(p,s)T^ab(p,s') \\ & +\sin\varphi(p)\mu_{ss'}b^\dagger(p,s)T^ad^\dagger(-p,s') \\ & -\sin\varphi(p)\mu_{s's}b(p,s)T^ad(-p,s')+\cos\varphi(p) \\ & \times(\vec{\sigma}\cdot p)^*_{ss'}d^\dagger(-p,s')T_ad(-p,s), \end{aligned} \tag{8}$$

where $\mu_{ss'}$ is the pion spin matrix,

$$\mu_{ss'}=\begin{bmatrix} 0 & 1 \\ -1 & 0 \end{bmatrix}. \tag{9}$$

It is obvious from the inspection of this equation that for non vanishing $\varphi(p)$ we get Bogolioubov anomalous contributions for Q_5^a. This fact alone allows us to implement the *sine qua non* condition for spontaneous symmetry breaking (in this case of chiral symmetry):

$$Q_5^a|0\rangle\neq 0, \quad [Q_5^a,H]=0. \tag{10}$$

When we apply this commutator to the new vacuum it is straightforward to see that the only nonzero contribution for $Q_5^a|0\rangle$ is provided by the anomalous term of Q_5^a which is none other than the composite operator for the pion creation. Then at the BCS level Eq. (10) implies that the pion mass must be zero. This is indeed the case when we solve the corresponding Salpeter equation for the pion [18,17,20]. As expected the π relative wave function turns out to be given by $\sin\varphi(k)$. Finally the nonanomalous terms of Q_5^a simply describe the $g_a\simeq\cos\varphi$ coupling of quarks to pions. Only in the case of the usual Fock space ($\varphi=0$) do we have that Q_5^a annihilates the empty vacuum.

Although the actual functional form of $\varphi_{[V]}$ may vary, depending on the interaction details, the mechanism described above is general: Any Bogolioubov (canonical) transformation on the Fock space of the creation and annihilation operators can be cast as a rotation through an angle $\varphi/2$ and this fact together with the invariance of the field operator Ψ under these transformations produces a corresponding counterrotation on the spinorial basis. This is enough for the Q_5^a to acquire an anomalous term going like $\sin\varphi$, the pion wave function.

In terms of the Fock space operators, the Hamiltonian becomes

$$H=H_2+H_4,$$

$$H_2=\int d^3k \;\; E(k)[b^\dagger_{fsc}(\mathbf{k})b_{fsc}(\mathbf{k})+d^\dagger_{fsc}(\mathbf{k})d_{fsc}(\mathbf{k})],$$

$$H_4=\frac{1}{2}\int d^3p\; d^3k\; d^3q\, V(\mathbf{q})\left(\frac{\lambda^a_{c_1c_2}\lambda^a_{c_3c_4}}{4}\right)$$

$$\times\sum_{j,l=1}^{4}:\Theta^j_{c_1c_2}(\mathbf{p},\mathbf{p}+\mathbf{q})\Theta^l_{c_3c_4}(\mathbf{k},\mathbf{k}-\mathbf{q}):. \quad (11)$$

The two terms H_2 and H_4 have been normal ordered. The normal ordering of the potential energy operator introduces self-energy terms, already included in H_2, which contribute to the quark energy $E(k)$:

$$E(k)=A(k)\sin\varphi(k)+B(k)\cos\varphi(k),$$

$$A(k)=m_q+\frac{2}{3}\int\frac{d^3p}{(2\pi)^3}\,V(\mathbf{k}-\mathbf{p})\sin\varphi(p),$$

$$B(k)=k+\frac{2}{3}\int\frac{d^3p}{(2\pi)^3}(\hat{\mathbf{k}}\cdot\hat{\mathbf{p}})V(\mathbf{k}-\mathbf{p})\cos\varphi(p) \quad . \quad (12)$$

There are also constant terms arising from the normal ordering of both the kinetic and the potential energy operators. Their sum yields the energy of the vacuum condensate.

As for H_4, and after summing over the indices j and l, we get ten different terms which can be cast as combinations of four vertices Θ^j:

$$\Theta^1_{c'c}(\mathbf{p},\mathbf{p}')\equiv u^\dagger_{s'}(\mathbf{p}')u_s(\mathbf{p})\;\; b^\dagger_{fs'c'}(\mathbf{p}')b_{fsc}(\mathbf{p}),$$

$$\Theta^2_{c'c}(\mathbf{p},\mathbf{p}')\equiv -v^\dagger_{s'}(\mathbf{p}')v_s(\mathbf{p})\;\; d^\dagger_{fsc}(-\mathbf{p})d_{fs'c'}(-\mathbf{p}'),$$

$$\Theta^3_{c'c}(\mathbf{p},\mathbf{p}')\equiv u^\dagger_{s'}(\mathbf{p}')v_s(\mathbf{p})\;\; b^\dagger_{fs'c'}(\mathbf{p}')d^\dagger_{fsc}(-\mathbf{p}),$$

$$\Theta^4_{c'c}(\mathbf{p},\mathbf{p}')\equiv v^\dagger_{s'}(\mathbf{p}')u_s(\mathbf{p})\;\; d_{fs'c'}(-\mathbf{p}')b_{fsc}(\mathbf{p}) \quad . \quad (13)$$

For the kernel H_4 we can use the Ward identity [24,20] to obtain, at least at the BCS level, the so-called *mass gap equation*

$$A(k)\cos\varphi(k)-B(k)\sin\varphi(k)=0 \quad , \quad (14)$$

which defines the chiral angle $\varphi(k)$. Alternatively we can find the minimum of the vacuum energy in terms $\varphi(k)$. These two methods yield the same mass gap equation.

III. BOUND STATE EQUATIONS

In Ref. [17] we studied the light quark mesons, and have shown that the negative energy component of the wave function is only relevant for pseudoscalar mesons which play the role of the Goldstone boson when $m=0$. For quark or antiquark current masses bigger than a given scale, which depends on the strength of the particular confining potential used, we can neglect this negative energy component. This is the case for charmonium. In the case of the K meson, which corresponds to an intermediate case with a strange quark mass of the order of few tens of MeV, the negative energy wave function to turns out to be small (less than 30%) when compared with the corresponding positive energy component whereas in the case of free nucleons this negative energy component simply does not exist. Although there is in the K-N system a transition potential connecting the K positive energy wave function component to its negative counterpart, it contributes to the K-N scattering with the square of the ratio of these two wave function components and this amounts to a multiplicative factor of the order of 10% on top of the fact that this transition potential is weak. Therefore in K-N scattering we can discard, both for K and N, these negative energy components and the bound state equation can be simply written in the form

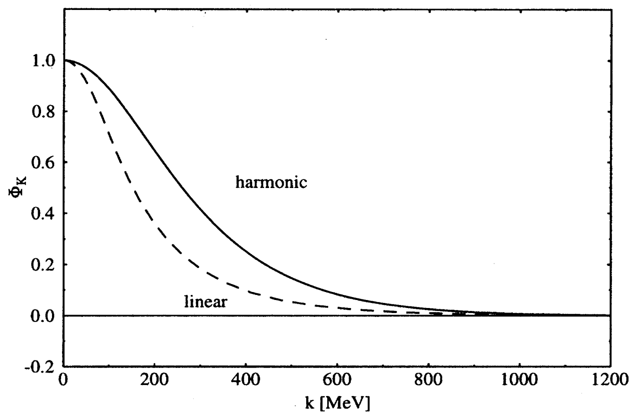

FIG. 1. K S-wave functions for harmonic and linear potentials in arbitrary units.

$$H|\psi\rangle=M|\psi\rangle \quad , \quad (15)$$

where $|\psi\rangle$ is an eigenstate of the Hamiltonian, with mass M.

Here we report on our results for *bare* K and N, i.e., without coupled hadronic channels. Hence, we do not consider those vertices which create or annihilate light q-$\bar{q}$pairs. These diagrams contribute to the self-energies of the exterior hadronic legs and their net effect is to contribute with a negative shift of the respective bare masses towards the physical masses. Although this constitutes a small correction to the kaon mass, it is not so in the case of the nucleon [22]. Fortunately it is sufficient to have a consistent order of magnitude for the bare nucleon mass. This is due to the fact that the kaon probes essentially the bare component of the physical nucleon.

A. K meson

Disregarding the negative energy channel, we can write the general mesonic creation operator as

$$\Psi_m^\dagger = \int d^6p\,\delta(\mathbf{p}_1+\mathbf{p}_2)\psi(\mathbf{p}_1,\mathbf{p}_2)\ \chi_{f_1f_2s_1s_2}\ b^\dagger_{f_1s_1c}(\mathbf{p}_1)d^\dagger_{f_2s_2c}(\mathbf{p}_2)\ . \tag{16}$$

The one-quark part of the Hamiltonian, Eq. (11), acting on the meson states returns

$$H_2\Psi_m^\dagger|0\rangle = \int d^6p\,\delta(\mathbf{p}_1+\mathbf{p}_2)[E(p_1)+\bar{E}(p_2)]\psi(\mathbf{p}_1,\mathbf{p}_2)\chi_{f_1f_2s_1s_2}\ b^\dagger_{f_1s_1c}(\mathbf{p}_1)d^\dagger_{f_2s_2c}(\mathbf{p}_2)|0\rangle\ . \tag{17}$$

Because in general the quark current masses can be different, their corresponding kinetic energy $E(p)$ may be different; i.e., different flavors lead to different chiral angles. Therefore we use the notation $E(p)$ $[\bar{E}(p)]$ for one of the quarks [antiquarks] involved in the microscopic scattering. The same is true of the spinors u and v which also depend on the chiral angle; consequently, we will use $\bar{v}$ for the second vertex in the potential.

Only one of the ten terms in H_4 connects mesonic positive energy states with themselves, namely, the term

$$:\Theta^1_{c_1c_3}(\mathbf{p},\mathbf{p}')\bar{\Theta}^2_{c_2c_4}(\mathbf{k},\mathbf{k}'):=-u^\dagger_{s_1}(\mathbf{p}')u_{s_3}(\mathbf{p})\bar{v}^\dagger_{s_4}(\mathbf{k}')\bar{v}_{s_2}(\mathbf{k})b^\dagger_{f_1s_1c_1}(\mathbf{p}')d^\dagger_{f_2s_2c_2}(-\mathbf{k})d_{f_2s_4c_4}(-\mathbf{k}')b_{f_1s_3c_3}(\mathbf{p})\ . \tag{18}$$

When the corresponding part of H_4 operates on the meson state the result is

$$\begin{aligned}H_4\Psi_m^\dagger|0\rangle = -\frac{4}{3}\chi_{f_1f_2s_3s_4}\int d^6p\ d^3q\,\delta(\mathbf{p}_1+\mathbf{p}_2)V(\mathbf{q})\psi(\mathbf{p}_1-\mathbf{q},\mathbf{p}_2+\mathbf{q})u^\dagger_{s_1}(\mathbf{p}_1)u_{s_3}(\mathbf{p}_1-\mathbf{q})\bar{v}^\dagger_{s_4}(-\mathbf{p}_2-\mathbf{q})\bar{v}_{s_2}(-\mathbf{p}_2)\\ \times b^\dagger_{f_1s_1c}(\mathbf{p}_1)d^\dagger_{f_2s_2c}(\mathbf{p}_2)|0\rangle.\end{aligned} \tag{19}$$

The bound state equation is obtained from (17) and (19),

$$[M-E(k)-\bar{E}(k)]\chi_{f_1f_2s_1s_2}\phi(\mathbf{k}) = -\frac{4}{3}\int d^3q\ V(\mathbf{q})[u^\dagger_{s_1}(\mathbf{k})u_{s_3}(\mathbf{k}-\mathbf{q})\bar{v}^\dagger_{s_4}(\mathbf{k}-\mathbf{q})\bar{v}_{s_2}(\mathbf{k})]\chi_{f_1f_2s_3s_4}\phi(\mathbf{k}-\mathbf{q})\ , \tag{20}$$

where $\phi((\mathbf{p}-\mathbf{p}')/2)\equiv\psi(\mathbf{p},\mathbf{p}')|_{\mathbf{p}+\mathbf{p}'=0}$. With the negative energy channel excluded, this equation coincides with the Salpeter equation for mesons.

With the harmonic potential it is simple, starting from (20) to obtain a second order differential equation for the K S-wave function,

$$\left\{\frac{d^2}{dk^2}+M-E(k)-\bar{E}(k)-\frac{\varphi'^2(k)+\bar{\varphi}'^2(k)}{4}+\frac{\sin\varphi(k)\ \sin\bar{\varphi}(k)-1}{k^2}\right\}\nu(k)=0\ . \tag{21}$$

In this last equation all momenta, energy, and masses are given in units of $(4/3)^{1/3}K_H$. $\nu(k)$ represents the reduced K S-wave function. This equation can be solved using the numerical method of Ref. [17]. For the linear potential the derivation of this equation is far more complicated and we now get, for the $^1S_0$ mesonic bound states, an integro-differential equation instead of the simple differential equation of Eq. (21):

$$\begin{aligned}&[E_q+\bar{E}_q]\Phi_q-\frac{2k_l^2}{3\pi}\int_0^\infty dk\,\frac{2k^2}{(q^2-k^2)^2}\{[(1+S\varphi_k)(1+S\varphi_q)(1+S\overline{\varphi_k})(1+S\overline{\varphi_q})]^{\frac{1}{2}}[(1-S\varphi_k)(1-S\varphi_q)(1-S\overline{\varphi_k})(1-S\overline{\varphi_k})]^{\frac{1}{2}}\}\\&\times\Phi_k+\frac{-2k_l^2}{3\pi}\int_0^\infty dk\left[\frac{k}{2q}+\frac{k^2+q^2}{(q^2-k^2)^2}+\frac{\ln\left|\frac{q+k}{k-q}\right|}{2q^2}\right]\{[(1+S\varphi_k)(1+S\varphi_q)(1-S\overline{\varphi_k})(1-S\overline{\varphi_q})]^{\frac{1}{2}}+[(1-S\varphi_k)(1-S\varphi_q)\\&\times(1+S\overline{\varphi_k})(1+S\overline{\varphi_q})^{\frac{1}{2}}]\}\ \ \Phi_k=M\Phi_q\,,\end{aligned} \tag{22}$$

where for instance $S\varphi_k$ stands for $\sin[\varphi(k)]$. Φ_k represents the $^1S_0$ mesonic wave function; k is the quark-antiquark momentum. In Fig. 1 we show two solutions for the kaon wave function, one for each of Eqs. (21) and (22). The corresponding potential strengths are given in Eq. (45).

B. Nucleon

The formalism used to derive the bound state equation for mesons can be easily generalized to bound states of three quarks. As was already mentioned the wave functions of baryons have no contribution from negative energy channels. Furthermore, in this paper we will restrict our treatment to baryons with quarks of the same current mass, leading to only one chiral angle φ, the same dispersion relation $E(p)$ for the three quarks, and only one set of spinors u in the vertices Θ. We will also restrict the baryonic wave function of the nucleon to the simplest S-wave configuration, and discard, in what this paper is concerned, coupled channels which means that we will be considering bare nucleon masses rather than the pion-dressed physical masses. It turns out that typically the nucleon bare masses are a few hundred MeV larger than the physical masses. As we said this constitutes a reasonable approximation because the kaon is quite insensitive to this pion cloud and probes the bare nucleon which when seen as the bare component of the physical nucleon (with the right experimental mass) has a smaller size than the physical Nucleon.

Then, the creation operator for baryons has the form

$$\Psi_b^\dagger=\int d^9p\ \ \delta(\mathbf{p}_1+\mathbf{p}_2+\mathbf{p}_3)\ \psi(\mathbf{p}_1,\mathbf{p}_2,\mathbf{p}_3)\ \epsilon_{c_1c_2c_3}\ \chi_{f_1f_2f_3s_1s_2s_3}b^\dagger_{f_1s_1c_1}(\mathbf{p}_1)b^\dagger_{f_2s_2c_2}(\mathbf{p}_2)b^\dagger_{f_3s_3c_3}(\mathbf{p}_3)\ . \tag{23}$$

The anticommutation relations for the quark operators ensure antisymmetry as required by Pauli exclusion. Since the color part of the wave function, $\epsilon_{c_1c_2c_3}$, is completely antisymmetric, the flavor-spin-momentum wave function $\chi\psi$ can be taken to be symmetric.

The one-quark part of the Hamiltonian acting on the baryon state gives

$$H_2\Psi_b^\dagger|0\rangle=\int d^9p\ \ \delta(\mathbf{p}_1+\mathbf{p}_2+\mathbf{p}_3)[E(p_1)+E(p_2)+E(p_3)]$$
$$\times\psi(\mathbf{p}_1,\mathbf{p}_2,\mathbf{p}_3)\epsilon_{c_1c_2c_3}\chi_{f_1f_2f_3s_1s_2s_3}b^\dagger_{f_1s_1c_1}(\mathbf{p}_1)b^\dagger_{f_2s_2c_2}(\mathbf{p}_2)b^\dagger_{f_3s_3c_3}(\mathbf{p}_3)|0\rangle\ . \tag{24}$$

Without coupled channels, we have only to consider the following vertex product in the interaction

$$:\Theta^1_{c_1c_4}(\mathbf{p},\mathbf{p}')\Theta^1_{c_2c_5}(\mathbf{k},\mathbf{k}'):=u^\dagger_{s_1}(\mathbf{p}')u_{s_3}(\mathbf{p})u^\dagger_{s_2}(\mathbf{k}')u_{s_4}(\mathbf{k})b^\dagger_{f_1s_1c_1}(\mathbf{p}')b^\dagger_{f_2s_2c_2}(\mathbf{k}')b_{f_2s_4c_5}(\mathbf{k})b_{f_1s_3c_4}(\mathbf{p})\ , \tag{25}$$

which leads to

$$H_4\Psi_b^\dagger|0\rangle=-2\epsilon_{c_1c_2c_3}\chi_{f_1f_2f_3s_3s_4s_5}\int d^9p\ \ d^3q\,\delta(\mathbf{p}_1+\mathbf{p}_2+\mathbf{p}_3)V(\mathbf{q})\psi(\mathbf{p}_1-\mathbf{q},\mathbf{p}_2+\mathbf{q},\mathbf{p}_3)$$
$$\times[u^\dagger_{s_1}(\mathbf{p}_1)u_{s_3}(\mathbf{p}_1-\mathbf{q})u^\dagger_{s_2}(\mathbf{p}_2)u_{s_4}(\mathbf{p}_2+\mathbf{q})]b^\dagger_{f_1s_1c_1}(\mathbf{p}_1)b^\dagger_{f_2s_2c_2}(\mathbf{p}_2)b^\dagger_{f_3s_5c_3}(\mathbf{p}_3)|0\rangle\ . \tag{26}$$

The resulting bound state equation for baryons is

$$[M-3E(p_1)]\ \ \chi_{s_1s_2s_5}\ \ \psi(\mathbf{p}_1,\mathbf{p}_2,\mathbf{p}_3)$$
$$=-2\int d^3q\ \ V(\mathbf{q})\ \ [u^\dagger_{s_1}(\mathbf{p}_1)u_{s_3}(\mathbf{p}_1-\mathbf{q})u^\dagger_{s_2}(\mathbf{p}_2)u_{s_4}(\mathbf{p}_2+\mathbf{q})]\chi_{s_3s_4s_5}\psi(\mathbf{p}_1-\mathbf{q},\mathbf{p}_2+\mathbf{q},\mathbf{p}_3)\ , \tag{27}$$

with $\mathbf{p}_1+\mathbf{p}_2+\mathbf{p}_3=0$, for any flavor indices in the function χ. As in the case of mesons, Eqs. (21), (22), the potentials defined in (3) lead to the following differential equations:

harmonic

$$-\frac{d^2(k\ \Phi)}{dk^2}+\left[2k\cos(\varphi)-\frac{\varphi'^2}{2}-\frac{\cos(\varphi)^2}{k^2}+\frac{2[1-\sin(\varphi)]^2}{3k^2}\right](k\Phi)\ \ =\ \ \frac{2}{3}\,M(k\Phi), \tag{28}$$

linear

$$k\cos[\varphi(k)]\Phi(k)-\frac{2k_l^2}{2\pi}\ \int_0^\infty dq\ \frac{4q^2}{(q^2-k^2)^2}\left[\Phi(q)-\frac{\sin[\varphi(q)]}{\sin[\varphi(k)]}\ \ \Phi(k)\right]$$
$$-\frac{2k_l^2}{3\pi}\ \int_0^\infty dq\left[\frac{q\cos[\varphi(k)-\varphi(q)]}{k(q-k)^2}+\frac{q\cos[\varphi(k)+\varphi(q)]}{k(q-k)^2}-\frac{\ln\left|\dfrac{k+q}{q-k}\right|}{k^2}\cos[\varphi(k)]\cos[\varphi(q)]\right][\Phi(q)-\Phi(k)]$$
$$+\frac{4k_l^2}{9\pi}\int_0^\infty dq\left[-\frac{1}{k^2}+\frac{(k^2+q^2)\ln\left|\dfrac{k+q}{q-k}\right|}{2k^3q}\right]\{1-\sin[\varphi(k)]\}\{1-\sin[\varphi(q)]\}\Phi(q)=\frac{2M}{3}\ \ \Phi(k), \tag{29}$$

where Φ represents the quark wave function inside the nucleon. In Fig. 2 we plot the solutions of Eqs. (28) and (29) for the parameters of Eq. (45). We can see that for the same nucleon bare mass we obtain a much larger nucleon core in the case of the linear confining potential than in the harmonic case.

C. Quark kernels

The bound state equations (21), (22), (28), and (29) resemble Schrödinger equations with effective spin-spin interactions. However, all of these interactions have been derived from a *single* potential term of the Hamiltonian, and contain the "same" information of the chiral angle: for mesons,

$$-\frac{4}{3}\int d^3q\; V(\mathbf{q})[u^\dagger_{s_1}(\mathbf{k})u_{s_3}(\mathbf{k}-\mathbf{q})\bar{v}^\dagger_{s_4}(\mathbf{k}-\mathbf{q})\bar{v}_{s_2}(\mathbf{k})]\cdots, \tag{30}$$

for baryons,

$$-\frac{2}{3}\int d^3q\; V(\mathbf{q})[u^\dagger_{s_1}(\mathbf{p}_1)u_{s_3}(\mathbf{p}_1-\mathbf{q})u^\dagger_{s_1}(\mathbf{p}_2)u_{s_3}(\mathbf{p}_2+\mathbf{q})]\cdots . \tag{31}$$

In what follows, we will only consider the hyperfine interaction. It corresponds to the effective $\vec{S}\cdot\vec{S}$ interaction: harmonic,

$$V_{ij}=\frac{\hat{\mathbf{p}}_\mathbf{i}\cdot\hat{\mathbf{p}}_\mathbf{j}}{p_ip_j}[1-\sin\varphi(p_i)][1-\sin\varphi(p_j)]\vec{S}_i\cdot\vec{S}_j\frac{\vec{\lambda}_i\vec{\lambda}_j}{4}, \tag{32}$$

linear

$$V_{ij}=\int_0^\infty dq\left[-\frac{1}{k^2}+\frac{(k^2+q^2)\ln\left|\frac{k+q}{q-k}\right|}{2k^3q}\right](1-\sin\varphi_k)$$
$$\times(1-\sin\varphi_q)\vec{S}_i\cdot\vec{S}_j\frac{\vec{\lambda}_i\vec{\lambda}_j}{4}. \tag{33}$$

At this stage it is important to emphasize the conclusions of Ref. [19]. It is the fact that these interactions act in a space given by the direct product of the SU(2) representation for the spin and another SU(2) representation for the E spin, the latter being necessary to accommodate the negative energy components of the Salpeter mesonic amplitudes, which allows for a small hyperfine potential *but still* responsible for the $\rho-\pi$ mass difference. This is a consequence of the special status of the pion as a Goldstone boson and does not depend on the actual form of the microscopic potential provided it supports spontaneous chiral symmetry breaking. The above kernels can be thought of as a dynamical translation of this symmetry requirement through their explicit dependence on the chiral angle. This, together with the question of hadronic sizes, is crucial to understand the K-N phase shifts.

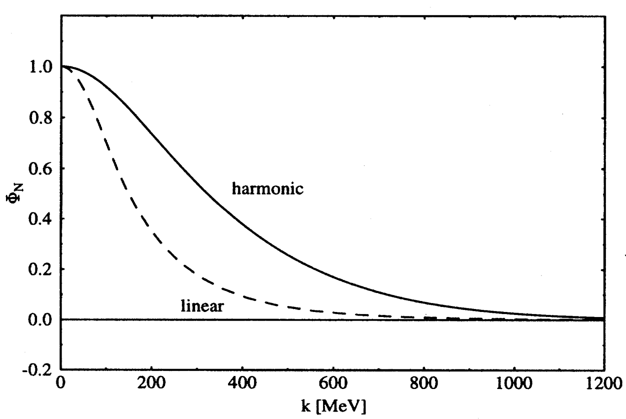

FIG. 2. N S-wave functions for harmonic and linear potentials in arbitrary units.

IV. K-N RGM EQUATION

For pure S-wave asymptotic hadron clusters we will only be needing the $\vec{S}\cdot\vec{S}$-type forces. The spin-orbit and tensorial forces, which are responsible for angular excitations, will not play a significant role in the low-energy elastic K-N S-wave phase shifts or, for that matter, the spin independent forces.

To study the K-N elastic scattering, we make use of the appropriated RGM equation [25] which, in turn, can be traced back to the Wick ordering of quark fields, and it is given by

$$\langle KN|(H-E)\mathscr{A}|KN\chi(R)\rangle=0,$$
$$\mathscr{A}=(1-3\mathscr{P}^{14})(1+\mathscr{P}_{KN}), \tag{34}$$

where the first quantization operator $\mathscr{A}$ stands for the antisymmetrizer; $\mathscr{P}^{14}$ forces the interchange of quark $1\in N(1,2,3)$ with quark $4\in K(4,5)$ and $\mathscr{P}_{KN}$ forces the interchange of clusters K and N as a whole. The coordinate representation of the kets $|K\rangle$ and $|N\rangle$ is given by the respective Bethe-Salpeter (BS) amplitudes in the spin representation. H and E stand, respectively, for the total Hamiltonian and energy. See Appendix A for the derivation of Eq. (34).

It is worthwhile to emphasize that the RG method, first introduced by Wheeler as a variational method solely based on a specific choice of a many-body trial wave function, can be entirely cast in second quantization formalism without resorting to the use of the exchange operators $\mathscr{P}^{ij}$. In other words, the RG method is the first quantization integro-differential equation we obtain when we solve, in field theory, the corresponding Dyson equation for bound state scattering. Equivalence between these two methods is achieved once we use BS amplitudes for the asymptotic bound states (instead of ordinary wave functions) together with the corresponding BS kernel for the RGM potential $V(q_iq_j)$ and the quark energy $E(k)$ that we obtain when solving the mass gap equation. Then, to describe the K-N scattering, it suffices to use the RG method with the kaon and the nucleon represented by the corresponding Salpeter amplitudes which are, respectively, the solutions of Eqs. (21), (28) for the harmonic potential or the solutions of Eqs. (22), (29) for the linear case. For the quark free Hamiltonian we use the $E(k)$ of expression (12). Then the Hamiltonian of Eq. (34) is simply given by the sum of the quark free Hamiltonians $E(k_i)$ plus the sum of all q_i-q_j kernels of expression (32) or (33). In this way we ensure that our calculation of K-N scattering is fully consistent with the requirements of spontaneous chiral symmetry breaking.

In turn, from Eq. (34) it is straightforward to deduce the associated Schrödinger equation

$$[(T_1+T_2-E_R)(1+\sigma|\Phi\rangle\langle\Phi|)+v|\Phi\rangle\langle\Phi|]|\chi\rangle=0,$$

$$\sigma|\Phi\rangle\langle\Phi|=\langle KN|3\ \mathscr{P}^{14}|KN\rangle,$$

$$v|\Phi\rangle\langle\Phi|=\langle KN|\sum_{ij;\ i\in K,j\in N}V_{ij}|KN\rangle. \tag{35}$$

In general v and σ are matrices associated with the spatial excitations of the asymptotic clusters. For ground states they are c numbers (see Appendixes B and C for a guide in calculating these numbers). They also depend on the isospin channel we are considering and are given in Eq. (38). Within each of the microscopic potentials studied in this work, both the kaon BS amplitude and the three-quark BS component of the nucleon wave function are, to a good approximation, given by the ground state harmonic oscillator wave function Φ^α with the same string constant α which coincides with the inverse radius of the nucleon.

It is convenient to use $|\Psi\rangle=[1+\sigma|\Phi\rangle\langle\Phi|]|\chi\rangle$ instead of $|\chi\rangle$. They yield the same phase shifts but it is much simpler to work with $|\Psi\rangle$. We have

$$|\Psi\rangle=|k\rangle\Big/\left(1-G_0\frac{v|\Phi\rangle\langle\Phi|}{1+\sigma}\right),$$

$$G_0=\frac{1}{E-T}. \tag{36}$$

$|k\rangle$ represents the free plane wave with momentum k. $|\Psi\rangle$ can be solved to give

$$|\Psi\rangle=|k\rangle+G_0\mathscr{T}|k\rangle,$$

$$\mathscr{T}=|\Phi\rangle\frac{v\ \ /(1+\sigma)}{1-\langle\Phi|G_0|\Phi\rangle v\ \ /(1+\sigma)}\langle\Phi|. \tag{37}$$

$\mathscr{T}$ is the T matrix. Then, the phase shifts are given by $\delta_0=\arg\mathscr{T}$(on mass shell). We have

$$I=0:\quad \sigma=0,\qquad v=-\frac{\mathscr{V}_{00}}{3};$$

$$I=1:\quad \sigma=-\tfrac{1}{3},\quad v=-\frac{7\mathscr{V}_{00}}{9};$$

$$\mathscr{V}_{00}=\langle\Phi|V_{ij}|\Phi\rangle. \tag{38}$$

And we see that in terms of Ψ it is simple to obtain the associated S-wave K-N effective potential V_I:

$$V_I=v\ \ /(1+\sigma),$$

$$V_I=\left(-\frac{\mathscr{V}_{00}}{3},-\frac{7\mathscr{V}_{00}}{6}\right),\quad I=(0,1). \tag{39}$$

Finally the isospin-dependent K-N scattering lengths a_I are simply given by

$$a_I=\frac{1}{\alpha}\ \frac{4\pi\mu V_I}{\alpha^2+4\pi^{\frac{1}{2}}\mu V_I}, \tag{40}$$

where μ is the reduced mass of the K-N system. For instantaneous interactions this expression is absolutely general.

V. RESULTS AND DISCUSSION

We have seen that the Salpeter equation provides an alternative and equivalent way of finding the pion wave function (and indeed all other quark bound states of the theory). The sizes of all these bound states will be similar and related to the potential strength which constitutes, together with the current quark masses, the only existing scales of the model. Therefore we can establish a link between the bare sizes of the hadrons and the extent of the chiral condensation. The details may vary depending on the particular form of the interaction but this self-consistent link, ensured by the mass gap equation, is generic. In particular the size of the bare nucleon is approximately the same as the size of the pion. This link can be written as

$$\langle\bar{\psi}\psi\rangle=-\frac{3}{\pi^2}\int_0^\infty dkk^2\sin(\varphi), \tag{41}$$

where $\sin(\varphi)$ is the pion wave function. We can parametrize this function as

$$\sin(\varphi)=e^{-k^2/\alpha^2} \tag{42}$$

to obtain a simple expression relating the bare size of the hadrons and the quark condensate,

$$\alpha=-\sqrt{\pi}(4\langle\bar{\psi}\psi\rangle/3)^{\frac{1}{3}}. \tag{43}$$

The accepted literature-average value of the quark condensate is $(-250\ \mathrm{MeV})^3$ which yields $\alpha\simeq 500$ MeV.

Next we choose to fix the potential strengths K_H (harmonic) and K_L (linear) as to give the same value for the bare nucleon mass m_N which we know to be larger than its physical counterpart by hundreds of MeV. This difference is a consequence of the coupling to $N\pi$ channels which considerably lowers the bare mass. A fairly independent model [22] puts this shift at $(-300,-400)$ MeV. Some time ago we did, for the quadratic potential, a thorough calculation of the ρ mass negative shift due to pion coupling [16]. We also found it to be of order of -400 MeV. A complete calculation of the physical nucleon mass, including the $N\pi$ channels will be even more involved but unnecessary since it suffices to have an order of magnitude for this shift. It happens that in the nucleon case, and for the *same parameters* used in the ρ calculation, this shift should be somewhat larger than in the ρ, because there are more diagrams for the $\langle N|\pi N\rangle$ coupling than for $\langle\rho|\pi\pi\rangle$. Therefore we expect a somewhat larger negative shift for the nucleon at around -500 MeV. So we make an educated guess for the nucleon bare mass to be 1500 MeV. The picture for the nucleon which emerges from this class of models is not dissimilar of that provided by the chiral bag model: a small nucleon core surrounded by a pion cloud. This bare nucleon mass is consistent with a mean radius of $\simeq 0.4$ fm, about one-half of the electromagnetic mean square radius, which does not differ too much from the cuttoff of 450 MeV already quoted in Chew's paper [1]. Moreover the bare $\Delta-N$ mass difference $\delta_{\Delta N}$ is simply given by

$$m_\Delta - m_N = -\mathscr{V}_{00}. \tag{44}$$

To have this bare nucleon mass we must set $K_H=408$ MeV and $K_L=492$ MeV.

At this stage it is important to point out that the question of obtaining a correct f_π is strongly connected both with the question of the nucleon core size and a covariant description of the quark potential. With our relatively small size for the nucleon bare wave function, necessary to obtain a reasonable K-N scattering length, we obtain a f_π of around 40 MeV as compared to usual value of 20 MeV quoted in the literature [18], which is obtained using bare hadrons. The importance of considering π-N coupled channels lies in the fact that now we are forced to raise the potential strength in order to obtain the correct hadron spectrum and this fact alone improves f_π noticeably. Admittedly this value falls short of the experimental value of 90 MeV. However, it should be stressed that f_π is very sensitive to the ratio of positive to negative E-spin energies of the pion. Horvat *et al.* [18], using a covariant description of the same microscopic potential and still without considering coupled channels, found an $f_\pi \simeq 34$ MeV. Therefore it seems probable that taking into consideration both these effects, covariance of the potential together with π-N coupled channels, will bring a very reasonable result for f_π.

Next, with these values for K_H and K_L and using Eqs. (38), (42), and (43) we can obtain the following values for $-\mathscr{V}_{00}$, and α:

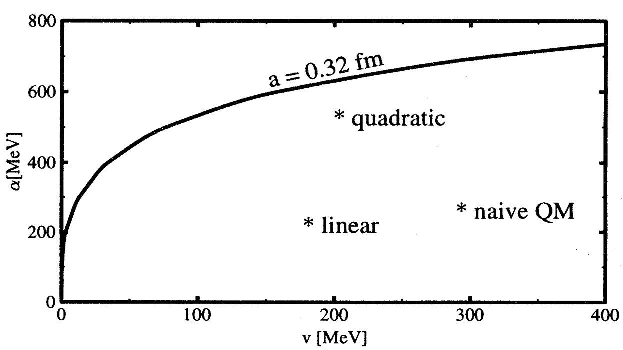

FIG. 3. The positions of linear, quadratic, and naive quark model in the plane defined by the inverse nucleon radius α versus the hyperfine potential strength ν. The curve where the experimental K-N scattering lengths are reproduced is also shown.

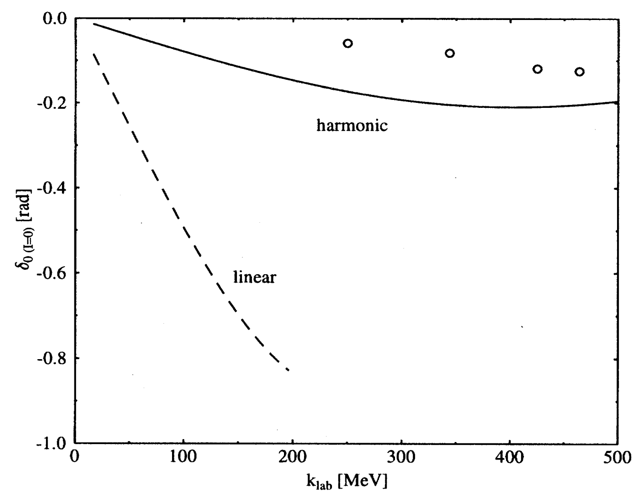

FIG. 4. $I=0$, S-wave K-N phase shifts for the harmonic (solid line) and linear potential (dashed line). The experimental data are represented by circles.

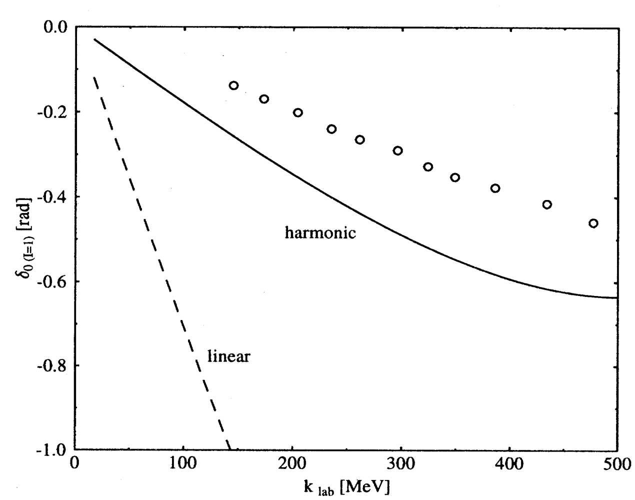

FIG. 5. $I=1$, S-wave K-N phase shifts for the harmonic (solid line) and linear potential (dashed line). The experimental data are represented by circles.

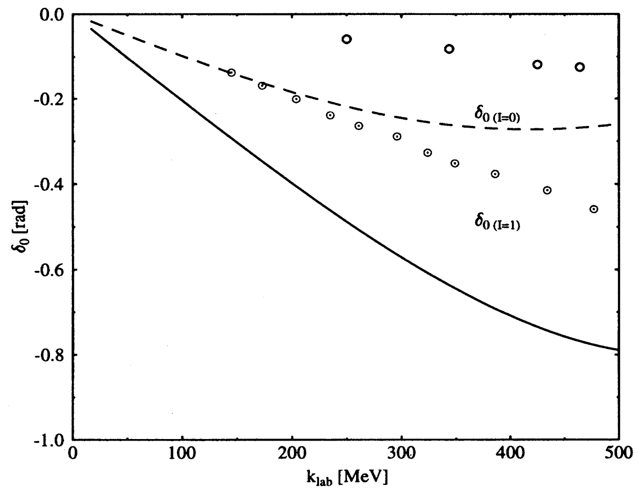

FIG. 6. K-N S-wave phase shifts with χSB turned off as compared with the experimental values.

model	harmonic	linear
$-\mathscr{V}_{00}$	$0.49K_H(200\ \text{MeV})$	$0.67K_L(180\ \text{MeV})$
α	$1.23K_H(500\ \text{MeV})$	$0.73K_L(210\ \text{MeV})$
$\delta_{\Delta N}$	200 MeV	180 MeV.

(45)

The effect of coupled channels should also contribute to the physical Δ-N mass difference. In Ref. [22] this contribution is set to (100–200) MeV.

From Eq. (40) it is simple to obtain the elastic $I=1,0$ K-N ratio for the scattering lengths,

$$\frac{a_{I=1}}{a_{I=0}} \simeq \frac{V_1}{V_0} \simeq 3.5, \tag{46}$$

in good agreement with experiment. Now if we use the physically correct $I=1$ K-N scattering length of 0.32 fm in Eq. (40) we obtain a relation between α and $\mathscr{V}_{00}$ allowing us to characterize several quark models as it is done in Fig. 3.

From Fig. 3 it is clear that the naive quark model is bound to fail to reproduce these scattering lengths no matter which parameters we might use. This is due to the fact that in the naive model $\mathscr{V}_{00}$ and α are fixed, respectively, by the experimental $\Delta-N$ mass difference and the inverse electromagnetic radius of the nucleus. It turns out that this yields a much too large scattering length a_I. The experimental scattering length can only be reproduced for smaller $\mathscr{V}_{00}$ and larger α. This is precisely what spontaneous χSB does. We require much less hyperfine splitting, maintaining at the same time a strong πN coupling. As for the linear confining potential it yields a relatively large nucleon and a small chiral condensate. Therefore it should not come as a surprise that in this case we are, for all hadronic phenomena other than the pion mass, closer to the naive quark model and, therefore, the associated K-N phase shifts should become worse.

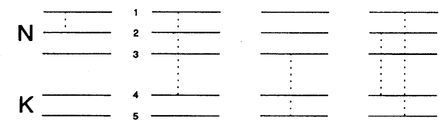

FIG. 7. Examples of interaction diagrams contributing to the S matrix of the K-N system.

For the $I=0;1$ S-wave phase shifts see Figs. 4 and 5. For the quadratic potential the theoretically obtained phase shifts turn out to be quite reasonable, the more so because they strongly depend on the chiral angle which in turn is obtained by solving the mass gap equation. This is not so in the linear case where we found quite large (negative) phase shifts. This result could be antecipated from Fig. 3. The linear potential only supports a small quark condensation and produces relatively bigger bare nucleon radius. To see the influence of the chiral condensation in the K-N phase shifts it suffices to turn off the mecanism for χSB and plot the resulting phase shifts. This we have done in Fig. 6. for the harmonic case which gave the results closest to the experimental ones. We obtained quite negative phase shifts. Of course in the linear case the effect of turning off the χSB would have made the resulting phase shifts still more negative.

APPENDIX A: THE RGM EQUATION

See Fig. 7 for examples of the diagrams we have to consider for the K-N system. These diagrams can be divided into several classes such as any two diagrams of a given class must commute. If we do not consider quark exchange, the S matrix for this system is simply given by

$$S_{KN} = g + \mathscr{T}\ S_{KN},$$

$$\begin{aligned} \mathscr{T} = \sum & \text{ of all irreducible diagrams of Fig. 7} \\ -\sum & \text{ of the product of all pairs of commuting diagrams} \\ +\sum & \text{ of all triple products of commuting diagrams} \cdots . \end{aligned} \tag{A1}$$

In Eq. (A1) we denote by g the the product of the five free quark propagators,

$$g = G_{q1} G_{q2} G_{q3} G_{q4} G_{\bar{q}5}. \quad \text{(A2)}$$

The mass gap equation provides a key ingredient to the evaluation of Eq. (A1). It allows the separation of the quark free Feynman propagator $\langle \overline{\psi_{fc}(\mathbf{x})\psi_{fc}(\mathbf{x})} \rangle$ into two separate propagators, one for quark fields $Q(x)$ and another for the antiquark fields $AQ(x)$,

$$\psi_{fc}(\mathbf{x}) = Q_{fc}(\mathbf{x}) + AQ_{fc}(\mathbf{x}),$$

$$Q_{fc}(\mathbf{x}) = \int \frac{d^3p}{(2\pi)^{3/2}} u_s(\mathbf{p}) b_{fsc}(\mathbf{p}),$$

$$G_Q(\mathbf{x}_1 - \mathbf{x}_2) = \langle \bar{Q}_{fc}(\mathbf{x}_1) \quad Q_{fc}(\mathbf{x}_2) \rangle,$$

$$\langle \bar{\psi}_{fc}(\mathbf{x}_1) \quad \psi_{fc}(\mathbf{x}_2) \rangle = \langle \bar{Q}_{fc}(\mathbf{x}_1) \quad Q_{fc}(\mathbf{x}_2) \rangle + \langle \bar{A}Q_{fc}(\mathbf{x}_1) \quad AQ_{fc}(\mathbf{x}_2) \rangle, \quad \text{(A3)}$$

where $G_Q(\mathbf{x}_1 - \mathbf{x}_2)$ is the quark propagator. This a direct consequence from the fact that the mass gap can be understood as a diagonalization condition on the Feynman propagator, $\langle \bar{\psi}_{fc}(\mathbf{x}) \quad \psi_{fc}(\mathbf{x}) \rangle$, as it is depicted in Fig. 8. Upon integration in the energies flowing in the propagators G_{qi} we also find

$$g = \frac{i}{E - E_K - E_N}. \quad \text{(A4)}$$

Next, if we allow quark exchange (which corresponds to consider all the Wick orderings) we have, for the complete K-N quark free propagator,

$$\mathscr{A} = (1 - \mathscr{P}^{14} - \mathscr{P}^{24} - \mathscr{P}^{34})(1 + \mathscr{P}_{KN}),$$

$$G_{KN} = \mathscr{A} \quad g, \quad \text{(A5)}$$

where the so-called exchange operators $\mathscr{P}^{ij}$ are introduced to keep track of the Wick orderings. $\mathscr{P}_{KN}$ corresponds to the exchange of quark content of K and N as a whole. The operator $\mathscr{A}$ is the antisymmetrizer.

Now, with quark exchange, the Dyson equation for the S_{KN} matrix is

$$S_{KN} = G_{KN} + \mathscr{T} \quad S_{KN}. \quad \text{(A6)}$$

$\mathscr{T}$ has already been defined in Eq. (A1). Multiplying Eq. (A6) by GS_{KN}^{-1} we obtain

$$(1 - \mathscr{T}) S_{KN} = \mathscr{A} g. \quad \text{(A7)}$$

It can be shown with all generality that

$$S_{KN} = |\chi\rangle |N(1,2,3) \quad K(4,\bar{5})\rangle \frac{i}{E_\chi - E_K - E_N} \langle K(4,\bar{5}) N(1,2,3) | \langle \chi |, \quad \text{(A8)}$$

where χ represents the K-N relative motion and $|K\rangle$ and $|N\rangle$ stand for the Salpeter wave functions for the K and N. Substituting Eq. (A8) into Eq. (A6) we can obtain

$$H = E_K - E_N - \mathscr{T},$$

$$\langle N(q_1, q_2, q_3) K(q_4, \bar{q}_5) | \mathscr{A}(E - H) | K(q_4, \bar{q}_5) N(q_1, q_2, q_3) \rangle | \chi \rangle = 0, \quad \text{(A9)}$$

which is known as the RGM equation. H is symmetric in all quark indices and therefore $\mathscr{A}$ commutes with H which in turn allows us to write Eq. (34).

APPENDIX B: COLOR⊗FLAVOR⊗SPIN OVERLAPS

Antisymmetry of the nucleon wave function and the fact that it is a color singlet force us to to write the flavor⊗spin ⊗space wave function as a completely symmetric one. We make the (negligible) approximation of having a symmetric wave function for the direct product of flavor⊗spin. In principle we could have more complicated configurations but they would correspond to excited states of the nucleon and are not expected to contribute for the low-energy K-N scattering. Therefore we have

$$\Psi_{\text{flavor}\otimes\text{spin}\otimes\text{space}}(123) = \frac{1}{\sqrt{2}} (D_f D_s + F_f F_s) S(123), \quad \text{(B1)}$$

where $D_{f,s}, F_{f,s}$ stand for the mixed symmetry Yamanouchi symbols, D and F, respectively in flavor and spin space. Explicitly,

$$D^{\uparrow}_{\text{spin}} = \frac{1}{\sqrt{6}} (\downarrow\uparrow\uparrow + \uparrow\downarrow\uparrow - 2\uparrow\uparrow\downarrow),$$

$$F^{\uparrow}_{\text{spin}} = \frac{1}{\sqrt{2}} (\downarrow\uparrow\uparrow - \uparrow\downarrow\uparrow). \quad \text{(B2)}$$

$S(123)$ stands for a symmetric space wave function and the same for $F_{\text{flavor}}, D_{\text{flavor}}$ provided we make the substitutions $\uparrow \to u, \downarrow \to d$ in the case of protons and $\uparrow \to u, \downarrow \to -d$ in the case of the neutrons. The kaon wave functions we will be needing in this paper are

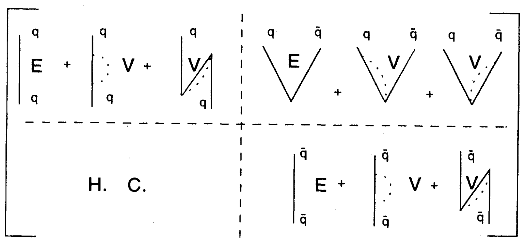

FIG. 8. Quark (antiquark) propagator before diagonalization.

$$K^{+}=u\bar{s}\frac{1}{\sqrt{2}}(\uparrow\downarrow-\downarrow\uparrow),$$

$$K^{0}=d\bar{s}\frac{1}{\sqrt{2}}(\uparrow\downarrow-\downarrow\uparrow). \tag{B3}$$

The total wave function, when projected in the appropriate isospin channel, is given by

$$I=1{:}K^{+}P,$$

$$I=0{:}\ \frac{1}{\sqrt{2}}(K^{+}N-K^{0}P). \tag{B4}$$

The factorization properties of both the nucleon and kaon wave functions in terms of (flavor⊗spin)⊗space allows for a considerable simplification when evaluating the various overlap kernels of Eq. (34). This is the more so because we can redraw all the Feynman diagrams with intercluster $V_{i,j}$ (i.e., $i\in K$; $j\in N$) to an equivalent diagram now with an intracluster insertion (in this case it is convenient, $i\in K$; $j\in K$). See Fig. 9 for an example. This fact allows us to completely disentangle the flavor⊗spin overlaps from the space overlaps, the latter being simple space norm kernels, i.e., space wave function expectations of the exchange operator $\mathscr{P}$ which can be readily solved using the graphical rules of Appendix C. As for the flavor⊗spin we have to evaluate not only norm kernels but also the contributions of the quark-quark potentials which, because they relate only to the kaon wave function are trivial to get.

1. Norm kernels

It is convenient to work with $\mathscr{P}^{34}$ which is diagonal in the F,D space for the quark numbering 123:nucleon,4$\bar{5}$:kaon. It should not matter as all the contributions must be the same regardless of the i(nucleon)j(kaon) quark pair. Therefore at the end of any calculation involving $\mathscr{P}^{34}$ it suffices to multiply the obtained results by 3, the number of all quark permutations acting in the K-N system to get the corresponding "physical" value.

Now, K being a spin singlet, and observing that

$$\vec{S}_i\cdot\vec{S}_j=\tfrac{1}{2}(\mathscr{P}^{ij}-\tfrac{1}{2}), \tag{B5}$$

we obtain

$$\langle FK|\mathscr{P}^{34}|FK\rangle_{\text{spin}}=\langle DK|\mathscr{P}^{34}|DK\rangle_{\text{spin}}=\tfrac{1}{2}. \tag{B6}$$

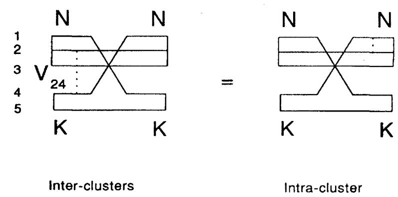

FIG. 9. Redrawing an intercluster interaction as an intracluster interaction.

For the flavor it is simpler to use the wave function explicitly. We get, for $I=(1,0)$,

$$\langle FK|\mathscr{P}^{34}|FK\rangle_I=(1,-1),$$

$$\langle DK|\mathscr{P}^{34}|DK\rangle_I=(\tfrac{1}{3},1). \tag{B7}$$

Putting everything together we finally get, for σ,

$$\sigma=\langle K\quad N|3\mathscr{P}^{34}|N\quad K\rangle,$$

$$\langle K\quad N|3\mathscr{P}^{34}|N\quad K\rangle=(\tfrac{1}{3},0),\quad I=(1,0). \tag{B8}$$

Finally, in color space the expectation value of $\langle 00|\mathscr{P}^{34}|00\rangle$ for color singlets is $\frac{1}{3}$.

2. Contributions from the hyperfine quark-quark potentials

We have four distinct types of contributions of V_{ij} insertions for the K-N scattering kernel $\mathscr{K}$:

$$\mathscr{K}=\langle N(1,2,3)\quad K(4,\bar{5})|\mathscr{P}^{34}\quad V_{ij}|N(1,2,3)\quad K(4,\bar{5})\rangle. \tag{B9}$$

To evaluate the kernels $\mathscr{K}$ we can choose the quark pairs $(ij)=(1,4),(3,\bar{5}),(3,4),(1,\bar{5})$. The other two possible quark pair contributions will be identical to one or another of the above four types.

We can describe these various contributions by the diagrams of Fig. 10. It can be shown that all of them are proportional to the kaon expectation value of the microscopic potential V_{ij},

$$\mathscr{K}\simeq\langle K|V_{(4,5)}|K\rangle,$$

$$\langle K|V_{(4,5)}|K\rangle=\langle\Phi^{\alpha}|\hat{V}|\Phi^{\alpha}\rangle, \tag{B10}$$

where Φ is the kaon Salpeter wave function, α the string constant, and $\hat{V}_{4,5}$ one of the potentials of Eqs. (32) and (33) amputated of the $S\cdot S\quad \lambda\cdot\lambda$ factor.

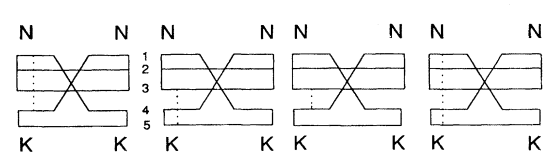

FIG. 10. Contributions to the potential kernel $\mathscr{K}$ of the RGM equation.

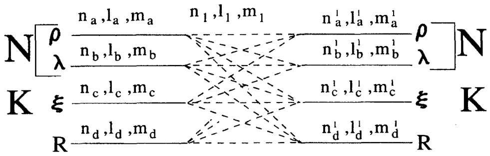

FIG. 11. Generic diagram for the graphical rules for space overlaps.

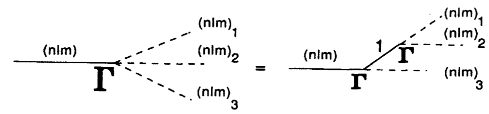

FIG. 12. Generic diagram for the vertex recoupling in the graphical rule diagrams.

This proportionality can be traced back to the freedom we have in redrawing the above diagrams.

Then, $\mathscr{V}_{00}$ is defined by

$$\mathscr{V}_{00}=\langle\Phi^{\alpha}|\hat{V}|\Phi^{\alpha}\rangle. \tag{B11}$$

We summarize the results:

type	weight	$I=1$	$I=0$
$(3,\bar{5})$	-6	$-\frac{1}{18}$	$-\frac{1}{6}$
$(1,4)$	-3	$-\frac{1}{3}$	0
$(1,\bar{5})$	-3	$-\frac{1}{3}$	0
$(3,4)$	-6	$-\frac{1}{18}$	$-\frac{1}{6}$,

where by "weight" we mean the number of distinct diagrams belonging to a particular type times the number of distinct quark permutations $-\mathscr{P}^{l,m}$ which is -3. We have to add the columns of $I=1$ and $I=0$ to obtain

$$I=0, \quad \nu=-\frac{\mathscr{V}_{00}}{3},$$

$$I=1, \quad \nu=-\frac{7}{9}\frac{\mathscr{V}_{00}}{}. \tag{B12}$$

APPENDIX C: GRAPHICAL RULES AND SPACE OVERLAPS

These rules [23] allow for an easy evaluation of overlap kernels induced by unitary nonlocal operators like, for instance, the exchange operator $\mathscr{P}^{ij}$. Although it is general and usable for an arbitrary number of clusters, each having an arbitrary number of particles, in the present paper we restrict the discussion to the concrete case of K-N. We are interested in evaluating,

$$\mathscr{O}=\langle N[(n,l,m)_{\rho};(n,l,m)_{\lambda}]K[(n,l,m)_{\epsilon}]\phi[(n,l,m)_{R}]|\mathscr{P}^{14}|\phi[(n'l'm')_{R}]K[(n',l',m')_{\epsilon}]N[(n',l',m')_{\rho};(n',l',m')_{\lambda}]\rangle. \tag{C1}$$

Above, (n,l,m) stand for the harmonic oscillator quantum numbers which provide a complete Hilbert space for space wave functions. ρ, λ, ϵ, and R stand for the appropriate Jacobi coordinates. They are defined in terms of the r_i coordinates as

$$\begin{bmatrix}\rho\\ \lambda\\ \epsilon\\ R\\ R_{C.M.}\end{bmatrix}=\begin{bmatrix}\frac{1}{\sqrt{2}} & \frac{-1}{\sqrt{2}} & 0 & 0 & 0\\ \frac{1}{\sqrt{6}} & \frac{1}{\sqrt{6}} & \frac{-2}{\sqrt{2}} & 0 & 0\\ 0 & 0 & 0 & \frac{1}{\sqrt{2}} & \frac{-1}{\sqrt{2}}\\ \frac{2}{\sqrt{30}} & \frac{2}{\sqrt{30}} & \frac{2}{\sqrt{30}} & \frac{-3}{\sqrt{30}} & \frac{-3}{\sqrt{30}}\\ \frac{1}{\sqrt{5}} & \frac{1}{\sqrt{5}} & \frac{1}{\sqrt{5}} & \frac{1}{\sqrt{5}} & \frac{1}{\sqrt{5}}\end{bmatrix}\begin{bmatrix}r_1\\ r_2\\ r_3\\ r_4\\ r_5\end{bmatrix}. \tag{C2}$$

In short $[\zeta]=[\Omega]\ [r]$. Knowing in the $[r]$ representation the matrix elements of $\mathscr{P}^{14}$, we obtain easily the corresponding elements in the $[\zeta]$ representation,

$$[\mathscr{P}^{14}]_{[\zeta]}=\Omega[\mathscr{P}^{14}]_{[r]}\Omega^T;[\mathscr{P}^{14}]_{([r],[\zeta])}=\left(\begin{bmatrix}0&0&0&1&0\\0&1&0&1&0\\0&0&1&1&0\\1&0&0&1&0\\0&0&0&1&1\end{bmatrix},\ \frac{1}{6}\begin{bmatrix}3&-\sqrt{3}&3&-\sqrt{15}&0\\-\sqrt{3}&5&\sqrt{3}&-\sqrt{5}&0\\3&\sqrt{3}&3&\sqrt{15}&0\\-\sqrt{15}&-\sqrt{5}&\sqrt{15}&1&0\\0&0&0&0&6\end{bmatrix}\right). \tag{C3}$$

The importance of the $[\mathscr{P}^{14}]_{[\zeta]}$ matrix elements is that these are the only numbers that are process dependent and that we have to know to be able to evaluate any space overlap kernel, to an arbitrary degree of precision no matter how complicated it may be. The number $\mathscr{O}$ and all the nonlocal kernels thereof obtained from Eq. (C1) by failing to integrate in one or more coordinates are given by the value of the diagram depicted in Fig. 11, where the dashed lines stand for the propagators, connecting vertices ij, contributing with

$$[[\mathscr{P}^{14}]_{[\zeta]}]_{ij}^{2n_a+l_a} \tag{C4}$$

and the typical vertex is depicted in Fig. 12, with the vertex

$$nlm\text{---}<\begin{matrix}n_a l_a m_a\\ n_a l_a m_a\end{matrix}.$$

In Fig. 11 sum over all the quantum numbers n_i,l_i,m_i flowing in the propagators except for the particular set of propagators we decided to amputate, $(\{(n_j,l_j,m_j)\cdots\})$, to obtain a corresponding set of separable kernels $\mathscr{O}(\{(n_j,l_jm_j)\cdots\})$ which are functions of those quantum numbers associated with the amputated propagators.

[1] G. Chew, Phys. Rev. **89**, 591 (1953).
[2] H. Stapp, Phys. Rev. **106**, 134 (1957).
[3] J. Schwinger, Ann. Phys. (N.Y.) **2**, 407 (1957).
[4] E. Sudarshan and R. Marshak, Phys. Rev. **109**, 1860 (1958); R. Feynmann and M. Gell-Mann, *ibid.* **109**, 193 (1958).
[5] J. Taylor, Phys. Rev. **110**, 1216 (1958); M. Gell-Mann and M. Levy, Nuovo Cimento **16**, 705 (1960).
[6] M. Gell-Mann, Phys. Lett. **8**, 214 (1964); J. Zweig, CERN report (unpublished).
[7] P. N. Bogolioubov, Ann. Inst. Henri Poincare **8**, 163 (1967).
[8] A. Chodos and C. B. Thorn, Phys. Rev. D **12**, 2733 (1975).
[9] S. Theberge, A. W. Thomas, and G. A. Miller, Phys. Rev. D **22**, 2838 (1980); A. W. Thomas, J. Phys. G **7**, L 283 (1981).
[10] S. Weinberg, Phys. Rev. Lett. **17**, 616 (1966); **18**, 188 (1967).
[11] E. A. Veit, B. K. Jennings, and A. W. Thomas, Phys. Rev. D **33**, 1859 (1986).
[12] E. A. Veit, A. W. Thomas, and B. K. Jennings, Phys Rev. D **31**, 2242 (1985).
[13] J. Bardeen, L. Cooper, and J. Schrieffer, Phys. Rev. **108**, 1175 (1957).
[14] Y. Nambu and G. Jona-Lasinio, Phys. Rev. **122**, 345 (1961); **124**, 246 (1961).
[15] P. Bicudo and J. Ribeiro, Z. Phys. C **38**, 453 (1988).
[16] P. Bicudo and J. Ribeiro, Phys. Rev. D **42**, 1635 (1990).
[17] P. Bicudo and J. Ribeiro, Phys. Rev. D **42**, 1611 (1990); **42**, 1625 (1990).
[18] A. Amer, A. Le Yaouanc, L. Oliver, O. Pène, and J-C. Raynal, Part. Fields, **17**, 61 (1983); A. Le Yaouanc, L. Oliver, O. Pène, and J-C. Raynal, Phys. Rev. D **29**, 1233 (1984); A. Le Yaouanc, L. Oliver, S. Ono, O. Pène, and J-C. Raynal, *ibid.* **31**, 137 (1985); P. Bicudo, Phys. Rev. Lett. **72**, 1600 (1994); R. Horvat, D. Kekez, D. Klabucar, and D. Palle, Phys. Rev. D **44**, 1584 (1991).
[19] P. Bicudo, G. Krein, J. Ribeiro, and J. Villate, Phys. Rev. D **45**, 1673 (1992).
[20] S. Adler and A. C. Davis, Nucl. Phys. **B244**, 469 (1984); R. Horvat, D. Kekez, D. Palle, and D. Klabucar, Zagreb Report No. ZTF-93-9-R, 1993 (unpublished); Y. Dai, Z. Huang, and D. Liu, Phys. Rev. D **43**, 1717 (1991).
[21] R. Bhaduri, L. Cohler, and T. Nogami, Nuovo Cimento **65A**, 376 (1981); B. Silvestre-Brac, J. Carbonell, and C. Gignoux, Phys. Lett. B **179**, 9 (1986); I. Bender, H. Dosh, H. Pirner, and H. Kruse, Nucl. Phys. **A414**, 359 (1984); D. Stanley and D. Robson, Phys. Rev. D **21**, 3180 (1980).
[22] A. W. Thomas and G. A. Miller, Phys. Rev. D **43**, 288 (1991).
[23] J. Ribeiro, Phys. Rev. D **25**, 2046 (1982); E. van Beveren, Z. Phys. C **17**, 135 (1983).
[24] H. Pagels, Phys. Rev. D **14**, 2747 (1976); **15**, 2991 (1977).
[25] J. Wheeler, Phys. Rev. **52**, 1083 (1937); **52**, 1107 (1937); J. Ribeiro, Z. Phys. C **5**, 27 (1980).